communications biology

Article

https://doi.org/10.1038/s42003-024-07055-y

RNA-binding protein IGF2BP1 is required for spermatogenesis in an age-dependent manner

Check for updates

Jiaqiang Luo[1,2,5], Chao Yang[3,5], Shuai Xu[1,2,5], Zhiyong Ji[4], Yuxiang Zhang[1], Haowei Bai[1], Zhiwen Deng[2], Jiayi Liang[2], Yuhua Huang[1], Erlei Zhi[1], Ruhui Tian[1], Peng Li[1], Fujun Zhao[1], Zhi Zhou[2] ✉, Zheng Li[1] ✉ & Chencheng Yao[1] ✉

Post-transcriptional regulation mediated by RNA binding proteins is crucial for male germline development. Insulin-like growth factor 2 mRNA-binding protein 1 (IGF2BP1), an RNA binding protein, is specifically expressed in human and mouse male gonads and is involved in manifold biological processes and tumorigenesis. However, the function of IGF2BP1 in mammalian spermatogenesis remains poorly understood. Herein, we generated an *Igf2bp1* conditional knockout mouse model using *Nanos3-Cre*. Germ cell deficiency of *Igf2bp1* in mice caused spermatogenic defects in an age-dependent manner, resulting in decreased numbers of undifferentiated spermatogonia and increased germ cell apoptosis. Immunoprecipitation-mass spectrometry analysis revealed that ELAV-like RNA binding protein 1, a well-recognized mRNA stabilizer, interacted with IGF2BP1. Single cell RNA-sequencing showed distinct mRNA profiles in spermatogonia from conditional knockout versus wide type mice. Further research showed that IGF2BP1 plays a vital role in the modulation of spermatogenesis by regulating *Lin28a* mRNA, which is essential for clonal expansion of undifferentiated spermatogonia. Thus, our results highlight the crucial effects of IGF2BP1 on spermatogonia for the long-term maintenance of spermatogenesis.

Spermatogonial stem cells (SSCs) are responsible for the continuous production of sperm throughout a man's life, ensuring fertility[1]. SSCs possess self-renewal and differentiation capacity and are regulated by orderly intrinsic gene expression[2,3]. RNA-binding proteins (RBPs) are a class of proteins that interact with RNA molecules, and play pivotal roles in post-transcriptional gene regulation[4]. The RBPs recognize and bind specific RNA sequences or structures, modulating RNA stability, splicing, localization, translation, and degradation[5]. Several studies have showed the pivotal functions of RBPs in regulating the maintenance and differentiation of SSCs. For instance, NANOS2 is an RBP involved in maintaining the primitive state of mouse SSCs by mediating direct translational repression of differentiation-related transcripts and inhibiting the activity of mammalian target of rapamycin complex 1 (mTORC1)[6]. The deleted in azoospermia-like (DAZL) protein regulates the expansion and differentiation of progenitor spermatogonia by orchestrating a broad translational program that regulates the expression levels of key proteins, including Lin-28 homologue A (Lin28a), forkhead box O1 (Foxo1) and Sal-like protein 4 (Sall4)[7]. These results indicate that RBPs are essential for the maintenance of SSCs and expansion of progenitor spermatogonia.

Insulin-like growth factor 2 mRNA-binding protein 1 (IGF2BP1) is a critical post-transcriptional regulator that exerts significant control over gene expression by binding with specific mRNA targets and contains four hnRNP-K homology domains and two RNA recognition motifs domains[8]. IGF2BP1 belongs to the IGF2BP family and plays an essential role in the regulation of target mRNAs related to metabolism, impacting diverse cellular processes such as stem cell maintenance and tumorigenesis[9,10]. It has been shown that IGF2BP1 regulates target mRNAs through distinct mechanisms, one mechanism involves IGF2BP1 binding to target mRNA, protecting it from degradation by endonucleases[11]. In another mechanism, IGF2BP1 associates with target mRNAs in RNA-induced silencing

[1]Department of Andrology, The Center for Men's Health, Urologic Medical Center, Shanghai Key Laboratory of Reproductive Medicine, Shanghai General Hospital, Shanghai Jiao Tong University School of Medicine, Shanghai, 200080, China. [2]School of Life Science and Technology, ShanghaiTech University, Shanghai, 201210, China. [3]Department of Urology, The First Affiliated Hospital With Nanjing Medical University, Nanjing, Jiangsu, 210029, China. [4]Center for Reproductive Medicine, The First Affiliated Hospital of Xiamen University, Xiamen, Fujian, 361003, China. [5]These authors contributed equally: Jiaqiang Luo, Chao Yang, Shuai Xu ✉e-mail: zhouzhi@shanghaitech.edu.cn; lizhengboshi@sjtu.edu.cn; yaochencheng@sjtu.edu.cn

complex-free complexes, inhibiting miRNA-mediated degradation of target mRNAs[12]. Recent studies revealed that IGF2BP1 promotes the expression of *SRF* by impairing the miRNA-directed decay of *SRF* mRNA and promoting the G1/S cell cycle transition[13,14]. IGF2BP1 also bound to the 3′-untranslated region (UTR) of *CD44*, *CTNNB1* and *MAPK4* mRNAs, inhibiting their degradation and stabilizing the mRNAs[8,15,16]. Interestingly, it has been reported that *Imp*, an ortholog of *Igf2bp1* in *Drosophila*, maintains germline stem cells (GSCs) by stabilizing *upd* mRNA in the *Drosophila* testis stem cell niche[17]. In humans, IGF2BP1 is highly expressed in the male reproductive system[18]. However, the in vivo function of IGF2BP1 in mammalian spermatogenesis, particularly regarding its age-related actions, remains inadequately characterized.

The current study integrated multiple approaches to query the biological and molecular roles of IGF2BP1 in spermatogenesis. We found that IGF2BP1 is specifically expressed in human and mouse spermatogonia. It was shown that *Igf2bp1* deficiency impaired spermatogenesis in an age-dependent manner, especially in 12-month-old conditional knockout (cKO) mice. Immunoprecipitation and mass spectrometric analysis revealed that ELAVL1, a well-recognized RNA stabilizer, is a potent co-factor of IGF2BP1. Furthermore, single-cell RNA-sequencing (scRNA-seq) revealed that *Igf2bp1* deficiency in mice resulted in the downregulation of the expression of key regulators of SSC maintenance. Coupling with RNA immunoprecipitation-sequencing (RIP-Seq), we identified target mRNAs of IGF2BP1 that are enriched in "gene silencing", "RNA localization" and "regulation of gene expression, epigenetic", including *Lin28a*, *Dnd1*, *Gfra1* and *Mov10*. In addition, immunofluorescence staining showed that IGF2BP1 and LIN28A exhibit simultaneous high expression in human seminoma tissues. Collectively, this study suggests that IGF2BP1 is a key RBP for the maintenance of spermatogonia in mammals and overexpression of IGF2BP1 is associated with human seminoma.

Results

IGF2BP1 is enriched in spermatogonia during human and mouse testicular development

Immunofluorescence staining was used to determine the expression of IGF2BP1 in both human and mouse testes. Human testes were derived from adult obstructive azoospermia (OA)-affected patients with normal spermatogenesis, and pre-pubertal (2- and 5-years of age) and peri-pubertal (8-year-old) children. In OA testes, IGF2BP1 was expressed in glial cell line-derived neurotrophic factor receptor alpha 1-positive ($GFRA1^+$) undifferentiated SSCs and ubiquitin C-terminal hydrolase L1-positive ($UCHL1^+$) spermatogonia, with high expression in cytoplasm (Supplementary Fig. 1a, b). However, the expression of IGF2BP1 rapidly decreased in c-KIT^+ differentiating spermatogonia (Supplementary Fig. 1c). The expression pattern was consistent during pre- and peri-puberty. In testes from 2-, 5- and 8-year-old donors, IGF2BP1 also co-localized with UCHL1 (Supplementary Fig. 2a–c).

In mouse testes, IGF2BP1 co-stained with mouse spermatogonia markers cadherin 1 (CDH1) and UCHL1, however it was undetectable in synaptonemal complex 3-positive ($SYCP3^+$) spermatocytes (Supplementary Fig. 3a–c). We also explored IGF2BP1 expression in mouse primary cultured GSCs and observed high expression of IGF2BP1 in the cytoplasm of cultured GSCs (Supplementary Fig. 3d). The conserved expression pattern suggested that IGF2BP1 is enriched in spermatogonia during human and mouse testicular development.

Igf2bp1 deficiency resulted in spermatogenic defects in an age-dependent manner in male mice

According to the UCSC genome browser and the UniProt server, IGF2BP1 was highly conserved in humans and mice (Supplementary Fig. 4a, b). To examine the function of IGF2BP1 during spermatogenesis in vivo, conditional knock-out (cKO, *Nanos3-Cre, Igf2bp1*$^{delete/flox}$) mice were generated by crossing *Igf2bp1*$^{delete/flox}$ mice with *Nanos3*-Cre recombinase transgenic mice (Fig. 1a). Western blotting and immunofluorescence demonstrated the complete depletion of IGF2BP1 in the *Igf2bp1* cKO mouse testes (Fig. 1b; Supplementary Fig. 5a).

At 8 months of age, *Igf2bp1* cKO mice exhibited significantly reduced testes volumes compared to wild type (WT) (Fig. 1c). The testis-to-body weight ratio showed no statistical difference at 2 months of age, began to decrease at 4 months, and followed an age-related pattern [12-month-old mice: 0.00086 ± 0.00017 (cKO) vs 0.00284 ± 0.00022 (WT)] (Fig. 1d). To test male fertility, 4-month-old WT and *Igf2bp1* cKO male mice were cohabited with WT female mice for 8 months, and the numbers of pups per litter generated by mating of 4- to 8-month-old and 8- to 12-month-old male mice were recorded. We found that the *Igf2bp1* cKO mice were fertile during 4- to 8-month-old, with no statistically significant difference in number of pups per litter compared to WT mice (Supplementary Fig. 5b). And *Igf2bp1* cKO male mice displayed reduced fertility compared with WT mice from 8 to 12 months of age. Among four *Igf2bp1* cKO male mice, two fathered no offspring from the age of 8 to 12 months (Supplementary Fig. 5b). Testicular histology analysis showed 4-month-old *Igf2bp1* cKO mice exhibited a higher proportion of abnormal seminiferous tubules with reduced germ cells versus WT mice (Fig. 1e). Furthermore, compared with 4-month-old *Igf2bp1* cKO mice, 8- and 12-month-old *Igf2bp1* cKO mice had more abnormal seminiferous tubules. Notably, up to 70% of seminiferous tubules were abnormal in 12-month-old *Igf2bp1* cKO mice [73.0% ± 9.8% (cKO) vs 2.3% ± 1.5% (WT)] (Fig. 1e, f). A significant reduction in sperm concentration was consistently observed from the caudal epididymis of *Igf2bp1* cKO compared with WT mice, accompanied by an extremely low sperm concentration in 12-month-old *Igf2bp1* cKO mice [3.9 ± 1.1 M/ml (cKO) vs 24.7 ± 1.4 M/ml (WT)] (Fig. 1g, h). There were no significant differences in serum testosterone levels between 12-month-old *Igf2bp1* cKO and WT mice (Supplementary Fig. 5c). These results revealed that loss of *Igf2bp1* in male mice resulted in spermatogenic defects in an age-dependent manner, indicating an indispensable role of IGF2BP1 in the maintenance of the male germ line with time.

Igf2bp1 deficiency reduced the pool size of undifferentiated spermatogonia in mice

To elucidate the testicular function of IGF2BP1, we analyzed spermatogenesis in 2-, 4-, 8- and 12-month-old *Igf2bp1* cKO and WT mice by immunofluorescence staining. Immunofluorescence staining for Sertoli cell marker sex determining region Y-Box 9 (SOX9) in testes showed that SOX9-positive cell numbers per tubule were similar in *Igf2bp1* cKO compared with WT mice of all ages (Fig. 2a; Supplementary Fig. 5d). Using the mouse testicular germ cell-specific antigen antibody TRA98, 8-month-old *Igf2bp1* cKO mice exhibited a higher proportion of abnormal testicular tubules, including tubules with massive loss of germ cells, as well as Sertoli cell only (SCO) tubules (Fig. 2a). The percent of SCO tubules increased significantly compared with WT mice in an age-dependent manner (Fig. 2b).

Promyelocytic leukemia zinc-finger (PLZF) is a common marker for undifferentiated spermatogonia, which comprises SSCs and progenitor germ cells, and KIT proto-oncogene receptor tyrosine kinase (c-KIT) is a common marker for differentiating spermatogonia. We counted the average number of PLZF-positive cells per seminiferous tubule from male mice of different ages. Notably, the average number of PLZF-positive cells per tubule significantly decreased in *Igf2bp1* cKO mice from 4-, 8- and 12-month-old compared with WT mice and showed a decreasing trend with age (Fig. 2c, d).

The average number of c-KIT-positive cells per tubule in 2-month-old *Igf2bp1* cKO mice showed no statistical difference, but it decreased in 4-, 8-, and 12-month-old *Igf2bp1* cKO mice and showed a decreasing trend with age (Fig. 2e). Also, we quantified the ratio of PLZF to c-KIT per tubule. The results showed that at 4-, 8- and 12-month-old, the PLZF/c-KIT ratio in cKO mice was lower compared to WT mice (Fig. 2f). Meanwhile, immunofluorescence staining of SYCP3 (components of the axial/lateral element) and PNA (a marker for the acrosome of sperm cells) showed that *Igf2bp1*

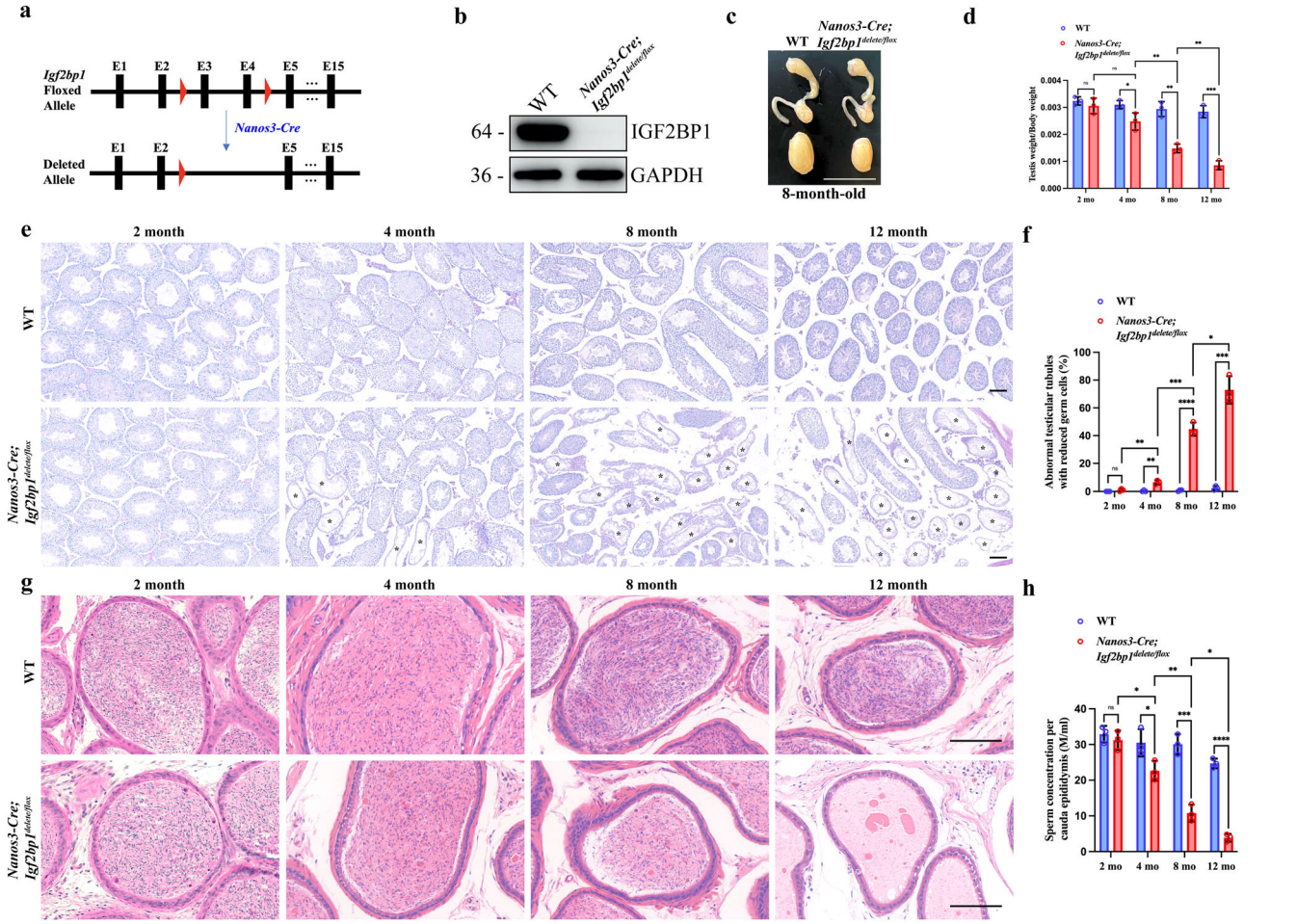

Fig. 1 | *Igf2bp1* depletion resulted in spermatogenic defects in an age-dependent manner in mice. a Schematic strategy for constructing the *Igf2bp1* conditional knock-out (cKO) mice. **b** Western blotting analysis of IGF2BP1 expression in the testes of wildtype (WT) and *Igf2bp1* cKO mice. GAPDH was used as a loading control. **c** The morphology of testes from 8-month-old WT and *Igf2bp1* cKO mice. Scale bar: 1 cm. **d** The testis-to-body weight ratios of 2-, 4-, 8- and 12-month-old WT and *Igf2bp1* cKO mice ($n = 3$). Bar graphs represent the means ± standard deviations. ns, not significant, $^{*}P < 0.05$, $^{**}P < 0.01$, $^{***}P < 0.001$. **e**, **f** Representative images of periodic acid-Schiff-stained testicular sections from 2-, 4-, 8- and 12-month-old WT and *Igf2bp1* cKO mice ($n = 3$). Scale bar: 100 μm. The *black asterisks* indicate abnormal seminiferous tubules. Bar graphs represent the means ± standard deviations. ns not significant, $^{*}P < 0.05$, $^{**}P < 0.01$, $^{***}P < 0.001$, $^{****}P < 0.0001$. **g** Representative images of hematoxylin-eosin stained cauda epididymal sections from 2-, 4-, 8- and 12-month-old WT and *Igf2bp1* cKO mice. Scale bar: 100 μm. **h** The sperm concentration per cauda epididymis from 2-, 4-, 8- and 12-month-old WT and *Igf2bp1* cKO mice ($n = 3$). Bar graphs represent the means ± standard deviations. ns, not significant, $^{*}P < 0.05$, $^{**}P < 0.01$, $^{***}P < 0.001$, $^{****}P < 0.0001$.

cKO testes have normal meiosis and spermiogenesis (Fig. 2g). In addition, TUNEL staining showed significantly increased germ cell apoptosis in 8-month-old *Igf2bp1* cKO mice compared with WT mice (Fig. 2h, i). These results suggested that IGF2BP1 is required to maintain the undifferentiated spermatogonia pool over time, and depletion of *Igf2bp1* destabilized the quantity of undifferentiated spermatogonia in mice.

IGF2BP1 interacted with mRNA stabilizer ELAVL1 in human and mouse testes

Immunoprecipitation and mass spectrometric analysis were used to investigate the partners of IGF2BP1 in human and mouse testes. After quality control, we identified 78 proteins in human and 73 proteins in mouse testes that potentially interacted with IGF2BP1, and 22 of them overlapped in both human and mouse testes (Fig. 3a). Gene Ontology (GO) analysis showed that these 22 proteins were enriched in the terms "regulation of mRNA stability", "mRNA binging" and "cytoplasmic ribonucleoprotein granule" (Fig. 3b). The protein-protein interaction network was constructed using the STRING database to find the hub gene. Interestingly, the results showed that ELAVL1 is the central protein in the protein-protein interaction network and has an extremely high combined score with IGF2BP1 (Fig. 3c; Supplementary Data 2).

Previous studies revealed that ELAVL1 is a highly conserved mRNA stabilizer involved in post-transcriptional gene regulation[19–23]. To study the interaction between IGF2BP1 and ELAVL1, we performed co-immunoprecipitation (co-IP) of IGF2BP1 and ELAVL1 using testis samples from patients with OA and mice. IGF2BP1 was able to efficiently pull down ELAVL1, indicating interaction between these two proteins in both human and mouse testes (Fig. 3d). Using HEK-293T cells transfected with plasmids containing 3× *Flag*-tagged *IGF2BP1* and *Myc*-tagged *ELAVL1*, co-IP showed that IGF2BP1 and ELAVL1 reciprocally interacted with each other with or without RNase A, establishing an in vitro interaction between the two proteins independent of RNAs (Fig. 3e). Furthermore, immunofluorescent staining of IGF2BP1 and ELAVL1 revealed their co-localization in the cytoplasm of human spermatogonia (Fig. 3f). These results suggested that ELAVL1 is a key interaction protein of IGF2BP1 involved in the regulation of target mRNA stability.

scRNA-seq demonstrated that IGF2BP1 deficiency altered mRNA profiles of spermatogonia

To explore the impact of IGF2BP1 on gene expression at single-cell resolution, we performed 10× Genomics scRNA-seq using 8-month-old *Igf2bp1* cKO and WT testes and obtained 6021 quality-controlled single cells.

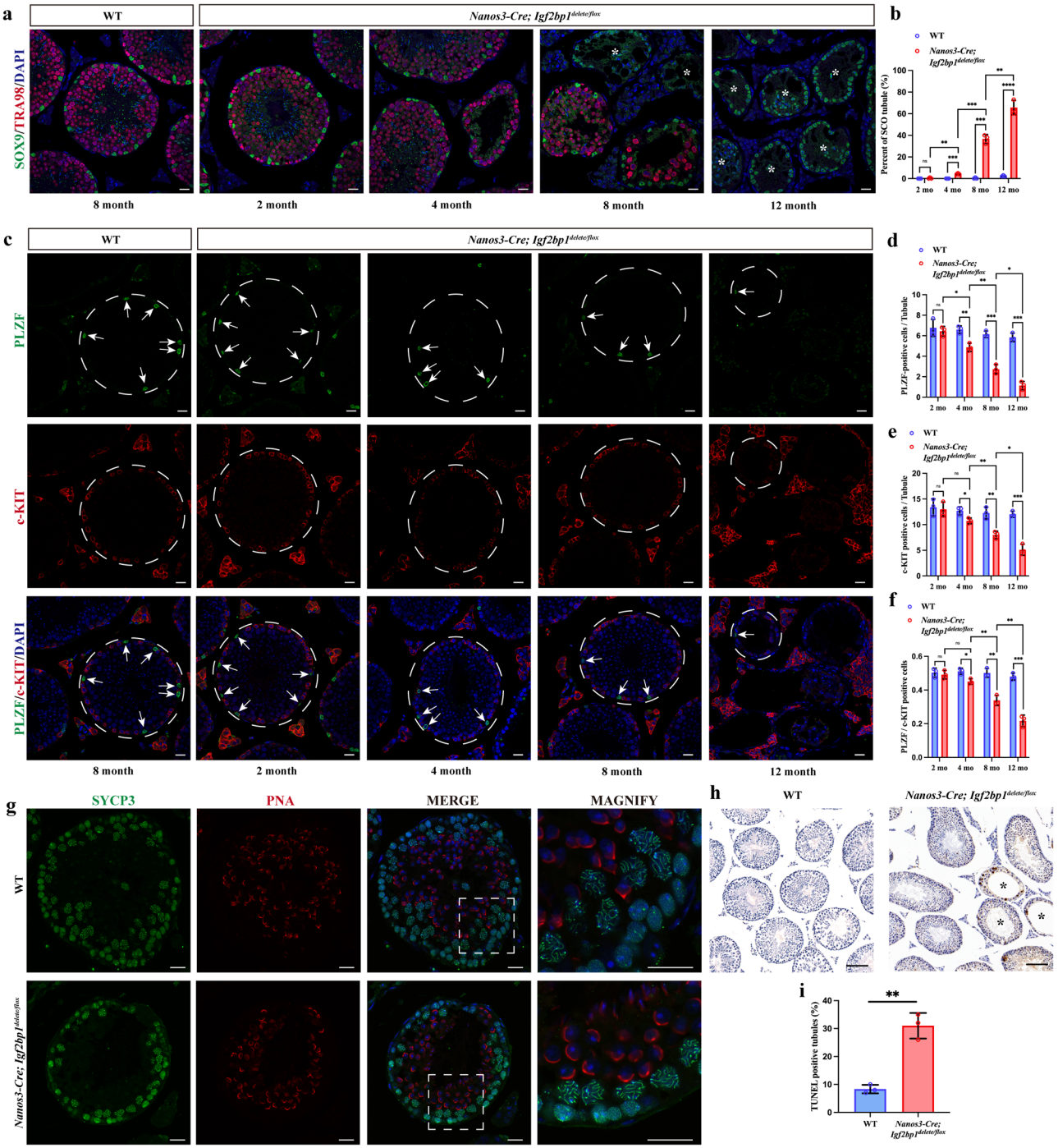

Fig. 2 | *Igf2bp1* depletion reduced the undifferentiated spermatogonia pool size in mice. a Immunostaining for SOX9 (Sertoli cell marker, green) and TRA98 (germ cell marker, red) in testes from 2-, 4-, 8- and 12-month-old wildtype (WT) and *Igf2bp1* conditional knock-out (cKO) mice. The *white asterisks* indicate Sertoli cell only (SCO) tubules. Scale bar: 20 μm. **b** Percentage of SCO tubules in 2-, 4-, 8- and 12-month-old WT and *Igf2bp1* cKO mice. Bar graphs represent the means ± standard deviations. ns not significant, $^{**}P < 0.01$, $^{***}P < 0.001$, $^{****}P < 0.0001$. **c** Immunostaining for PLZF (undifferentiated spermatogonia marker, green) and c-KIT (differentiating spermatogonia marker, red) in 2-, 4-, 8- and 12-month-old WT and *Igf2bp1* cKO mice. The *white arrows* indicate PLZF-positive cells. Scale bar: 20 μm. **d**–**f** The PLZF-positive cells (**d**), c-KIT-positive cells (**e**) and ratio of PLZF/c-KIT positive cells (**f**) per seminiferous tubule in 2-, 4-, 8- and 12-month-old WT and *Igf2bp1* cKO mice ($n = 3$; tubules per mouse, $n = 40$). Bar graphs represent the means ± standard deviations. ns, not significant, $^{*}P < 0.05$, $^{**}P < 0.01$, $^{***}P < 0.001$. **g** Immunostaining for SYCP3 (green) and PNA (red) in 8-month-old WT and *Igf2bp1* cKO mice. Scale bar: 20 μm. **h** Images of TUNEL staining of testicular sections from 8-month-old WT and *Igf2bp1* cKO mice. The *black asterisks* indicate TUNEL-positive tubules. Scale bar: 100 μm. **i** Percentage of TUNEL-positive tubules in 8-month-old WT and *Igf2bp1* cKO mice (mice, $n = 3$; tubules per mouse, $n = 40$). Bar graphs represent the means ± standard deviations. $^{**}P < 0.01$.

Dimensionality reduction and clustering analysis, combined with previously described known cell-type markers identified major germ cell populations covering the whole process of spermatogenesis, including A1: mainly undifferentiated spermatogonia, In-Bspg: differentiated spermatogonia, PL: pre-leptotene spermatocytes, L: leptotene spermatocytes, Z: zygotene spermatocytes, P: pachytene spermatocytes, D: diplotene spermatocytes, M1-M2: metaphase I and II spermatocytes, RS2-RS8: round spermatids and elongating spermatids (Fig. 4a, b). We utilized single-cell

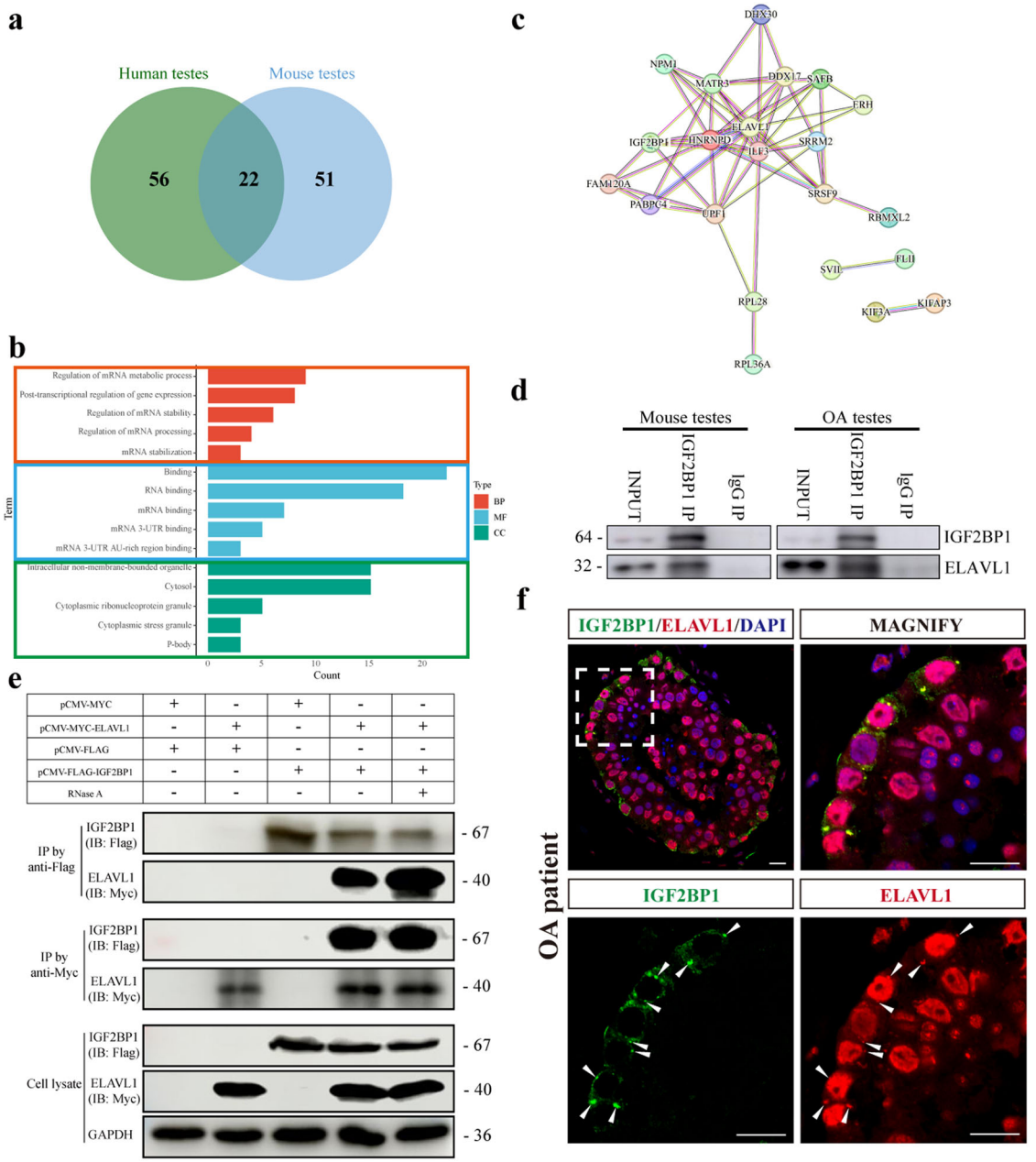

Fig. 3 | IGF2BP1 interacted with ELAVL1 in human and mouse spermatogonia. **a** Venn diagram showing the proteins enriched in IGF2BP1-immunoprecipitation (-IP) complexes in mouse and human testes, identified by mass spectrometry analysis. **b** Gene Ontogeny (GO) analysis of the overlapping targets of IGF2BP1. **c** STRING analysis of the proteins overlapping in the IGF2BP1-IP complex in mouse and human obstructive azoospermia testes. **d** Co-IP assay by anti-IGF2BP1 antibody showing the interaction between IGF2BP1 and ELAVL1 in both mouse and obstructive azoospermia testes. **e** Co-IP assay by anti-Myc or anti-Flag antibody showing the interaction between transfected 3× Flag-IGF2BP1 and Myc-ELAVL1 fusion proteins with or without RNase A treatment in HEK293T cells. **f** Co-localization of IGF2BP1 and ELAVL1 in human testis samples revealed by immunofluorescence staining (*white arrows*). Scale bar: 20 μm.

data to quantify the number and proportion of various germ cell types. Our analysis revealed that the number of all germ cell types significantly decreased in *Igf2bp1* cKO mice compared to WT (Fig. 4c). In terms of proportion, the In-Bspg and RS8 cell types appeared to have a higher proportion in *Igf2bp1* cKO mouse compared to WT (Fig. 4c). However, due to the uncertainties associated with single-cell enzymatic digestion and capture, accurately determining the proportions of different germ cell types using single-cell data may be challenging. To explore the transcriptional changes of *Igf2bp1* depletion in the A1 cluster (mainly undifferentiated spermatogonia), we conducted differentially expressed genes (DEGs) analysis of the transcriptome of A1 spermatogonia between WT and *Igf2bp1* cKO samples. Notably, 1627 genes were downregulated and 1622 genes were upregulated in A1 spermatogonia from *Igf2bp1* cKO versus WT mice (Fig. 4d). Previous studies have shown that IGF2BP1 can stabilize target mRNAs, such as *c-Myc* mRNA, through binding mRNA stabilizer ELAVL1[21]. Analysis of GO terms of downregulated genes in the *Igf2bp1* cKO compared with WT A1 spermatogonia groups revealed terms including "ribonucleoprotein complex biogenesis", "mRNA processing" and "gene silencing" (Fig. 4e). Meanwhile, we analyzed the upregulated genes in A1 and found that they are mainly associated with "establishment of protein localization to organelle", "ncRNA processing" and "RNA splicing" (Fig. 4f). Interestingly, key mRNAs that encode essential regulators of SSC proliferation and maintenance (*Lin28a*, *Dnd1*, *Gfra1*, and *Mov10*) were significantly decreased in the *Igf2bp1* cKO compared with WT

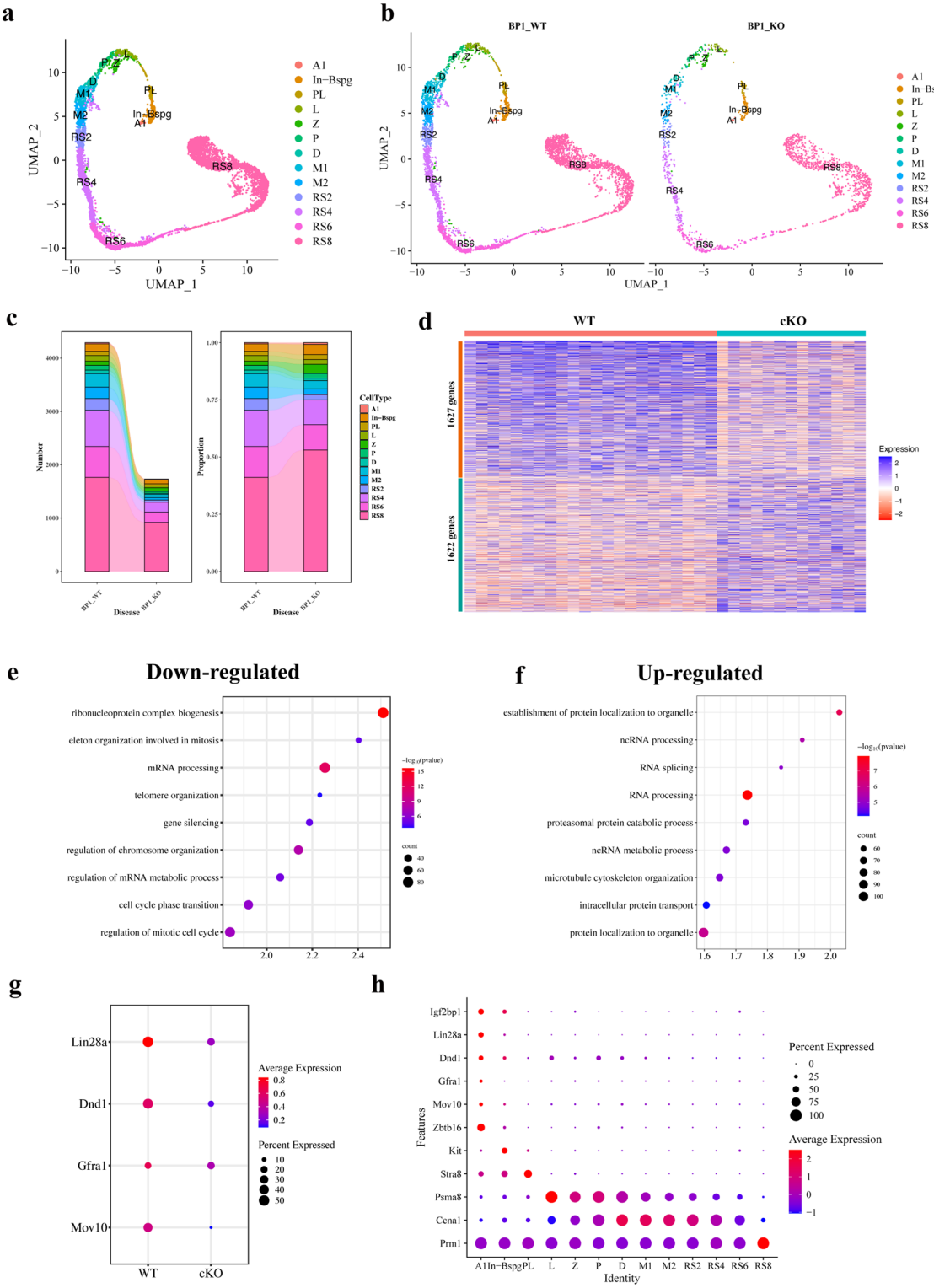

Fig. 4 | Overview of single-cell transcriptome profiling on *Igf2bp1* conditional knock-out (cKO) testes. a Uniform manifold approximation and projection (UMAP) plot of combined single-cell transcriptome from 8-month-old wild-type (WT) and *Igf2bp1* cKO mice testes. **b** UMAP plots of single-cell transcriptomes of 8-month-old WT or *Igf2bp1* cKO mice testes. **c** The stacked bar charts showing cell counts and proportions for different cell types in WT and *Igf2bp1* cKO mice. **d** Heatmap showing the differentially expressed genes (DEGs) for WT versus *Igf2bp1* cKO A1 cluster groups. Columns represent individual cells and rows represent DEGs. The gradient of two colors (red and blue) indicates low to high expression levels. **e**, **f** Gene Ontogeny (GO) analysis of the downregulated DEGs (**e**) and upregulated DEGs (**f**) in the *Igf2bp1* cKO versus WT A1 spermatogonia cluster groups. **g** Bubble diagram showing the expression levels of key mRNAs in WT and *Igf2bp1* cKO A1 clusters. The gradient of bubbles sizes indicates low to high percentage of expression in each cluster, and the gradient of two colors (blue and red) indicates low to high expression levels. **h** Bubble diagram showing the expression levels of key mRNAs in all clusters. The gradient of bubbles sizes indicates low to high percentage expression in each cluster, and the gradient of two colors (blue and red) indicates low to high expression levels.

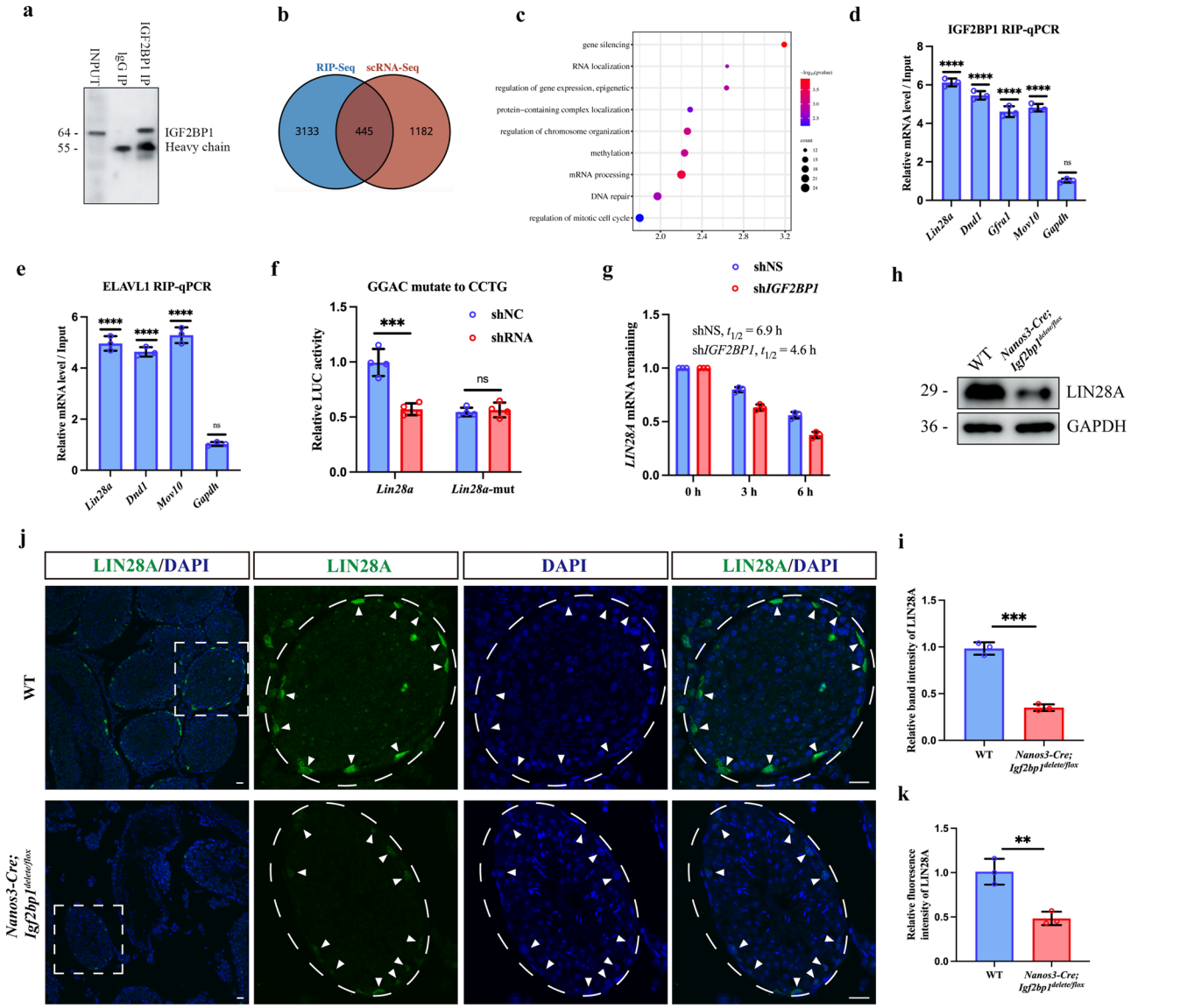

Fig. 5 | IGF2BP1 associated with mRNAs that encode essential regulators of spermatogonial stem cell (SSC) maintenance. a Immunoblot analysis of IGF2BP1 immunoprecipitation using cultured germline stem cells (GSCs). **b** Venn diagram showing the overlapping transcripts identified by RNA immunoprecipitation-sequencing (RIP-Seq) of GSCs and downregulated differentially expressed genes (DEGs) in the conditional knock-out (cKO) A1 spermatogonia cluster by single cell RNA-sequencing (scRNA-Seq). **c** Gene Ontology enrichment analysis of the overlapping transcripts identified by RIP-Seq of GSCs and downregulated DEGs in the cKO A1 cluster by scRNA-Seq. **d**, **e** RIP-qPCR analysis of IGF2BP1 (**d**) and ELAVL1 (**e**) potential targets in P10 mouse testes, with *Gapdh* as a negative control. Relative enrichment in IGF2BP1-IP and ELAVL1-IP was compared with input ($n = 3$). Bar graphs represent the means ± standard deviations. ns, not significant, $^{****}P < 0.0001$. **f** Luciferase reporter analysis demonstrating reduced activity of indicated reporters in *Igf2bp1*-knockdown (shRNA, red) compared with control HEK293T cells (shNC, blue). ns, not significant, $^{***}P < 0.001$. **g** Reducing *LIN28A* mRNA half-life by silencing *IGF2BP1* in Huh-6 cells. Bar graphs represent the means ± standard deviations. **h** Western blotting assay to compare the protein expressions of LIN28A between 8-month-old wildtype (WT) and *Igf2bp1* cKO mice. **i** The band intensity of LIN28A was normalized to GAPDH. $^{***}P < 0.001$. **j**, **k** Immunostaining of LIN28A in testes from 8-month-old WT and *Igf2bp1* cKO mice (mice $n = 3$; tubules per mouse, $n = 40$). Cell nuclei were stained with DAPI. The *white arrows* indicate LIN28A-positive cells. Fluorescence intensity of LIN28A was normalized to DAPI intensity. Bar graphs represent the means ± standard deviations. $^{**}P < 0.01$.

A1 spermatogonia clusters (Fig. 4g). Notably, these transcripts were also enriched in *Zbtb16* (*Plzf*)$^+$ A1 cluster spermatogonia, consistent with the expression of *Igf2bp1* (Fig. 4h). These results indicated that the depletion of *Igf2bp1* significantly altered the transcriptome of spermatogonia and downregulated key factors of SSC maintenance.

IGF2BP1 interacted with key mRNAs that encode essential regulators of SSC maintenance

To elucidate the function of IGF2BP1 in germ cells, we conducted sequencing of RNAs isolated by RNA immunoprecipitation sequencing (RIP-Seq) using IGF2BP1 antibody. Western blotting analysis confirmed successful immunoprecipitation of IGF2BP1 (Fig. 5a). Cultured mouse GSCs (~4 ×10^7) were used to pull-down RNAs, and 3578 genes were identified as putative targets, with 445 RNAs overlapping with down-regulated RNAs found in the A1 spermatogonia cluster of *Igf2bp1* cKO mice identified by scRNA-Seq (Fig. 5b). GO analysis of biological processes of these target RNAs showed that key RNAs are clustered in terms of "gene silencing", "RNA localization" and "regulation of gene expression, epigenetic" (Fig. 5c). Intriguingly, many target RNAs involved in these GO terms have been widely recognized as key regulators for the proliferation and

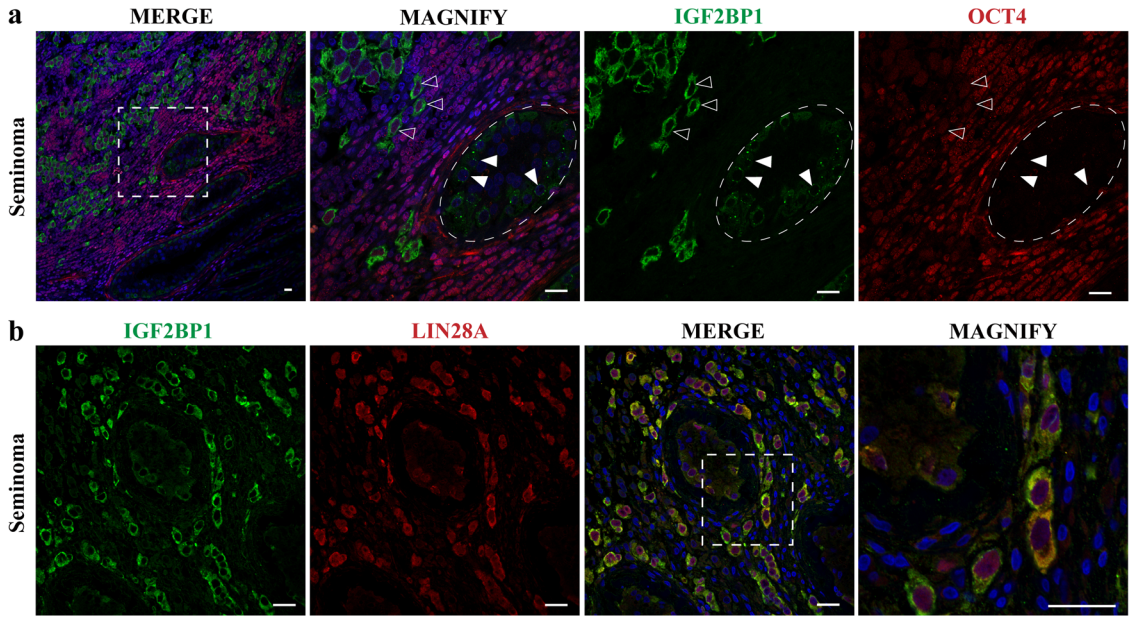

Fig. 6 | IGF2BP1 and LIN28A are highly expressed in human seminoma. a Co-staining of IGF2BP1 with the seminoma cell marker OCT4 in human seminoma and paracancer testicular tissues. The *white hollow arrows* indicate $OCT4^{+}$ cells and the *white solid arrows* indicate $OCT4^{-}$ cells. The white dashed-line oval indicates paracancer testicular tissues (seminiferous tubule). Scale bar: 20 μm. **b** Co-staining of IGF2BP1 with LIN28A in human seminoma. Scale bar: 20 μm.

maintenance of SSCs, including *Lin28a*, *Dnd1*, *Gfra1* and *Mov10*. RIP-qPCR validated the results of RIP-Seq of IGF2BP1 in mouse P10 testes (Fig. 5d). Additionally, to verify the interaction between ELAVL1 and these target mRNAs, we conducted RIP-qPCR for ELAVL1 in mouse P10 testes. The results demonstrated binding relationships between ELAVL1 and *Lin28a*, *Dnd1*, and *Mov10* (Fig. 5e).

LIN28A is an RNA-binding protein involved in pluripotency and stem cell maintenance and is strongly expressed in mouse and primate SSCs[24,25]. Testicular conditional depletion of *Lin28a* in mice resulted in impaired clonal expansion of undifferentiated spermatogonia[26]. To investigate whether *Lin28a* mRNA could be bound by IGF2BP1 via the motif (GGAC), WT and mutant type *Lin28a* 3′-UTR containing luciferase reporters were constructed and shRNA were used to efficiently knock down IGF2BP1 expression in the HEK293T cell line (Supplementary Fig. 5e, f). *IGF2BP1* knock-down resulted in downregulation of luciferase activity of the WT *Lin28a* 3′-UTR containing reporter (Fig. 5f). This downregulation was eliminated when the recognition motif GGAC was mutated to CCTG (Fig. 5f). Meanwhile, accelerated mRNA decay of *LIN28A* upon knockdown of IGF2BP1 was confirmed in Huh-6 cells (Fig. 5g, Supplementary Fig. 5g, h).

Furthermore, we examined the protein expression levels of LIN28A between WT and *Igf2bp1* cKO mouse testes using WB and immunofluorescence. The results showed that the expression of LIN28A in the testes of 8-month-old *Igf2bp1* cKO mice is significantly reduced compared to WT (Fig. 5h, i). Based on fluorescence intensity relative to DAPI, LIN28A expression was significantly reduced in 8-month-old cKO compared with WT mice (Fig. 5j, k). These results suggested that IGF2BP1 is associated with the maintenance of spermatogonia, potentially through the stabilization of target mRNAs, such as *Lin28a* mRNA.

IGF2BP1 and LIN28A are highly expressed in human seminoma

Immunofluorescence staining on human seminoma sections was used to investigate the expression pattern and correlation of IGF2BP1 and LIN28A in germ cell tumors. Human seminoma tissues were confirmed by histological analysis. Co-staining of IGF2BP1 with the seminoma cell marker octamer-binding transcription factor 4 (OCT4) showed that IGF2BP1 expression is significantly increased in $OCT4^{+}$ seminoma cells compared with $OCT4^{-}$ spermatogonia in human seminoma and paracancer testicular tissues (Fig. 6a). Furthermore, immunofluorescence staining showed that human seminoma tissues simultaneously express high levels of IGF2BP1 and LIN28A (Fig. 6b). These expression patterns suggested that the expression of IGF2BP1 and LIN28A may be correlated in human seminoma.

Discussion

Our research provided compelling evidence that IGF2BP1 has a critical role in mammalian spermatogenesis, particularly in the maintenance of SSCs. A novel mouse model showed that conditional depletion of *Igf2bp1* in germ cells lead to disruption of spermatogenesis in an age-dependent manner, with most seminiferous tubules becoming pathologically SCO in 12-month-old mice. Furthermore, we identified that ELAVL1 is a crucial co-factor of IGF2BP1 in testes, implicating a potential cooperative role in the regulation of mRNA stability during spermatogenesis. ScRNA-Seq and RIP-Seq analysis revealed that IGF2BP1 is largely associated with the maintenance of spermatogonia, potentially by regulating mRNA stabilization of essential regulators of SSC proliferation and maintenance, such as *Lin28a* mRNA. In addition, immunofluorescence staining showed that IGF2BP1 and LIN28A are synchronously expressed at high levels in human seminoma tissue.

The RBP IGF2BP1 plays a crucial role in recognizing and regulating the expression of key mRNAs. In lower organisms, such as *Drosophila*, the homolog of IGF2BP1, known as IMP, plays a critical role in the long-term maintenance of male GSCs, by counteracting endogenous small interfering RNAs to stabilize *upd* RNA in the stem-cell niche[17]. The current research showed aberrant spermatogenesis is increased in an age-dependent manner in *Igf2bp1* cKO mice, accompanied by a gradually declining testis-to-body weight ratio and an increasing number of SCO tubules from 4 to 12 months of age. Furthermore, PLZF-positive undifferentiated spermatogonia were markedly decreased in 4-, 8-, and 12-month-old *Igf2bp1* cKO mice. Meanwhile, TUNEL staining showed significantly increased germ cell apoptosis in 8-month-old *Igf2bp1* cKO mice compared with WT mice. We found that while most apoptotic cells are in the basal region of seminiferous tubules, specifically in spermatogonia, there are indeed instances of apoptosis observed in other germ cells. This observation appears inconsistent with the expected expression pattern of IGF2BP1. We hypothesize that this discrepancy may be related to the early transcription of key mRNAs of other germ cells in spermatogonia, which are subsequently regulated by IGF2BP1.

RIP-seq of IGF2BP1 revealed the presence of several crucial mRNAs, such as *Cdc45* and *Ccnd2*. However, additional experiments are required to validate and elucidate the molecular mechanisms underlying these observations. Subsequent IP-MS, STRING and co-IP assay analysis showed that ELAVL1 is a crucial co-factor for IGF2BP1 in the testis.

ELAVL1 is a highly conserved RBP involved in post-transcriptional gene regulation, significantly contributing to RNA stability[19]. ELAVL1 can bind to 3′-UTR AREs (AU-rich elements) and stabilize mRNAs by preventing their degradation[20,22,23]. Recent advancements have revealed that IGF2BP1 recruits ELAVL1 as co-factor to protect mRNAs from degradation[21]. Intriguingly, the present study also found that IGF2BP1 interacts with ELAVL1 in human and mouse testes and co-locates with ELAVL1 in the cytoplasm of spermatogonia. Therefore, these results indicate that IGF2BP1 may stabilize target mRNAs by recruiting ELAVL1 in mammalian spermatogenesis. In addition, spermatogenesis in *Elavl1*-deficient mice is arrested during meiosis and is characterized by a failure of spermatid elongation[27]. The differences in phenotypes between *Igf2bp1*-deficient mice and *Elavl1*-deficient mice are as follows. First, in *Igf2bp1*-deficient mice, abnormalities, including SCO tubules and a reduction in sperm count, began to appear as early as 4 months of age and worsen significantly with advancing age. *Elavl1*-deficient mice exhibit defects in delayed elongation of spermatids as early as 4 weeks of age, with compromised meiotic division observed from 9 weeks of age. Second, *Igf2bp1* depletion appeared to affect the long-term maintenance of spermatogonia, leading to age-dependent depletion of germ cells and eventual SCO tubules. On the other hand, *Elavl1* deficiency primarily caused extensive death of spermatocytes at meiotic divisions and failure of spermatid elongation. The phenotypic differences observed between IGF2BP1 and ELAVL1 deficiencies in mice can be attributed to several factors. One primary reason could be the broader expression range of ELAVL1 compared to IGF2BP1. ELAVL1 is expressed at higher levels in both spermatocytes and round spermatids, suggesting it plays a crucial role across various stages of spermatogenesis. Furthermore, the differences in observed phenotypes may also relate to the timing of phenotypic assessment in the mice. In *Igf2bp1*-deficient mice, abnormalities such as SCO tubules and reduced sperm count become evident as early as 4 months of age and worsen with advancing age. On the other hand, *Elavl1*-deficient mice show defects in spermatid elongation as early as 4 weeks, with compromised meiotic division observable from 9 weeks of age. However, the phenotypes of *Elavl1*-deficient mice have not been assessed in older mice, leaving a gap in understanding how these deficiencies manifest over a longer period. Thus, the distinct expression profiles and the timing of phenotypic observations likely contribute to the different impacts of IGF2BP1 and ELAVL1 deficiencies.

The RBPs fulfil their functions through regulation of target mRNAs in a post-transcriptional manner, and via synergistic action with other proteins. In the current study, scRNA-Seq identified 1627 downregulated RNAs in spermatogonia from 8-month-old testes *Igf2bp1* cKO versus WT testes. The application of RIP-Seq with GSCs identified more than 3000 potential targets of IGF2BP1. Because IGF2BP1 may regulate the stability of target mRNAs by recruiting ELAVL1, we examined the potential targets identified by RIP-Seq and the downregulated DEGs found in the spermatogonia A1 cluster of *Igf2bp1* cKO mice and identified 445 overlapping transcripts. Bioinformatics analysis indicated that these targets are enriched in the terms "gene silencing", "RNA localization" and "regulation of gene expression, epigenetic". Notably, transcripts regulating SSC maintenance were identified as the target mRNAs, including *Lin28a*, *Dnd1*, *Gfra1*, and *Mov10*. LIN28A is a developmental regulator known for its involvement in pluripotency and stem cell maintenance via repressed let-7 microRNAs[24,25]. Conditional depletion of *Lin28a* in the mouse male germline resulted in impaired clonal expansion of undifferentiated spermatogonia[26]. Dead end 1 (DND1) is a vertebrate-specific RNA-binding protein implicated in the survival of primordial germ cells and maintenance of spermatogonia. Murine *Dnd1* deficiency resulted in the depletion of both differentiating and undifferentiated spermatogonia[28]. DND1 binds the 3′-UTR region of mRNAs and destabilizes target mRNAs through direct recruitment of the CCR4-NOT deadenylase complex[29]. GFRA1 is a member of the glial cell line-derived neurotrophic factor receptor family and a common cell surface marker of undifferentiated spermatogonia[1]. *Gdnf*$^{+/-}$ mice showed depletion of the stem cell pool, resulting in SCO seminiferous tubules in older mice[30]. These findings showed that IGF2BP1 regulates the maintenance of spermatogonia through targeting these key genes.

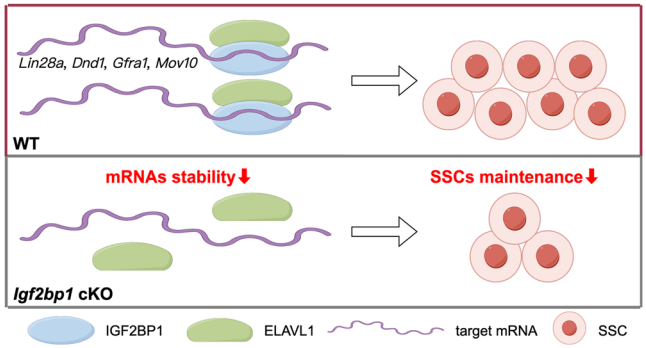

Fig. 7 | Diagram of proposed functions and mechanisms of IGF2BP1. IGF2BP1 is essential for the long-term maintenance of spermatogonia. Further experiments showed that mRNA stabilizer ELAVL1 is a crucial co-factor of IGF2BP1 in the testis and *Lin28a*, *Dnd1*, *Gfra1* and *Mov10* are crucial target mRNAs of IGF2BP1 in the regulation of spermatogonia.

Aberrant development in SSCs can lead to the formation of testicular germ cell tumors, specifically seminomas[31]. Seminomas resulting from the uncontrolled proliferation of spermatogonia highlighting the complex relationship between SSCs and testicular germ cell tumors. Interestingly, the present research showed that IGF2BP1 and LIN28A are highly expressed in seminomas. This suggests a potential balance in the expression of IGF2BP1 and LIN28A for spermatogenesis or seminomas. Deficiency of *Igf2bp1* may lead to decreased expression of LIN28A, consistent with the largely reduced SSC pool characterized by an abundance of SCO tubules in 12-month-old *Igf2bp1* cKO testes. Conversely, overexpression of IGF2BP1 may disrupt the normal regulation of LIN28A, leading to abnormal proliferation of SSCs and thereby the development of germ cell tumors.

In conclusion, our study provides compelling evidence for the critical role of IGF2BP1 in mammalian spermatogenesis, particularly in the maintenance of SSCs. The conditional depletion of *Igf2bp1* in germ cells resulted age-dependent and severe spermatogenic defects. Furthermore, co-IP revealed that ELAVL1 is a crucial co-factor of IGF2BP1 in the testis, implicating a potential cooperative role in the regulation of mRNA stability during spermatogenesis. Additionally, this study identified *Lin28a*, *Dnd1*, *Gfra1* and *Mov10* as crucial target mRNAs of IGF2BP1 in the regulation of spermatogonia (summarized in Fig. 7). Thus, our research expands the function of IGF2BP1 in regulating the long-term maintenance of mammalian spermatogenesis and provides new potential diagnostic and therapeutic targets for severe oligozoospermia, azoospermia and human seminoma in the future.

Materials and methods

Antibodies

The antibodies used for immunofluorescence and western blotting have been listed in Supplementary Data 3.

Human samples

Testicular tissue samples were obtained from three patients diagnosed with OA who had normal karyotypes, genotypes, and sex hormone levels, and exhibited normal spermatogenesis. Postoperative pathological examination showed that their Johnsen scores are not less than 9. Testicular tissues were obtained from children who underwent testicular biopsies or partial excision for the following indications: benign testicle mass (2 and 5 years of age) and contralateral testis to cryptorchidism (8-year-old), and children

patient's source in accordance with the previously described[32]. All children had normal karyotypes, genotypes, and sex hormone levels. Seminoma samples were confirmed by histological analysis. All participants in this study provided informed consent. The clinical data of the donors are summarized in Supplementary Data 4. This study was approved by the Ethical Review Committee of Shanghai General Hospital (Permit Number: 2020SQ199). All ethical regulations relevant to human research participants were followed.

Mouse model and cell line

Nanos3-Cre mice were maintained and used as a tool to conditionally induce gene depletion[33]. *Igf2bp1*$^{delete/flox}$ mice were used to delete *Igf2bp1* specifically in germ cells. All animals were maintained in a C57BL/6/MCH background. All mice were housed in a specific pathogen free animal facility under standard conditions by Gempharmatech Co., Ltd. We have complied with all relevant ethical regulations for animal use. All animal care and experiments adhered to the guidelines of the National Institutes of Health and were approved by the Animal Care Committee of Shanghai General Hospital. Supplementary Data 5 presents a list of the primers employed for genotyping *Igf2bp1* cKO mice. The HEK-293T and Huh-6 cells were cultured with DMEM medium containing 10% FBS at 37 °C and 5% CO_2 incubation. Primary GS cell lines were established and cultured as previously described[34]. Briefly, mouse embryonic fibroblasts (MEFs) derived from day 13.5 post-coitum mouse embryos were used as feeders. Postnatal day 5 C57BL/6 male mouse testes were aseptically removed and digested using 1 mg/ml collagenase IV (17104019, Thermo Fisher Scientific) and 1 mg/ml DNase I (90083, Thermo Fisher Scientific) to dissociate the tissue. The digested seminiferous tubules were mechanically dissociated into fragments using pipette tips. These fragments were then seeded into 12-well plates coated with 0.2% gelatin and cultured with 20 ng/ml rat glial cell line-derived neurotrophic factor (GDNF, 512-GF, R&D systems) for 18 h to promote initial colony formation. Each germline stem cell (GSC) colony was carefully blown off using a pipette and transferred to new plates coated with 0.2% gelatin. For the P1 generation, the cells were cultured in MEM-α/StemPro-34 medium (12561, GIBCO) supplemented with 20 ng/ml GDNF and 1 ng/ml mouse fibroblast growth factor 2 (FGF2; 450–33, Peprotech). The GSC colonies were then cultured in a feeder-free environment for 3–4 passages. During this period, somatic cell contamination decreased significantly, leaving only a thin layer of somatic cells. Once the somatic cells were sufficiently reduced, the GSCs were transferred to plates containing mitomycin C-treated MEFs. At this stage, the concentration of FGF2 was increased to the normal level of 10 ng/ml to support optimal GSC proliferation and maintenance. After the establishment of the GSC line, the cells can be passaged using 0.25% trypsin digestion, and the GDNF concentration can be reduced to 10 ng/ml.

Histological analysis

The tissues were fixed in 4% paraformaldehyde solution then dehydrated through a gradient of alcohol solutions, followed by infiltration with molten paraffin wax for subsequent sectioning. Cut 5-μm-thick sections were used for further histological staining. After deparaffinization and hydration, the testicular sections were subjected to periodic acid-Schiff staining, dehydration, blocking and scanning analysis. Similarly, the epididymis sections were subjected to hematoxylin-eosin staining according to the manufacturer's instructions.

Immunostaining of testicular tissues

Immunofluorescence staining was performed on 5 μm sections of human and mouse testicular samples. The sections were subjected to deparaffinization, rehydration and heat-mediated antigen retrieval in a 10 mM sodium citrate buffer solution (pH 6.0) at 105 °C for 15 min. After treatment with 5% donkey serum for 1 h at room temperature, individual sections were incubated overnight at 4 °C with a mix of diluted primary antibodies. Antigen detection was conducted using the appropriate combination of Alexa Fluor 488 and 594 secondary antibodies (Supplementary Data 3) for 1 h at room temperature in the dark. DAPI was used to label nuclei. Images were captured with an OLYMPUS confocal microscope (FV3000).

Plasmids construction

Plasmids pCMV-Myc-ELAVL1 and pCMV-3×Flag-IGF2BP1 were synthesized by amplifying specific coding sequences using PCR and then recombining into pCMV-Myc or pCMV-3×Flag vectors via the ClonExpress One Step Cloning Kit (C112, Vazyme). For knockdown of IGF2BP1, a DNA fragment encoding shRNA was synthesized in vitro and incorporated into the pGMLV-SC5 vector to produce the pGMLV-SC5-IGF2BP1 shRNA plasmid, which was purchased from Genomeditech Co., Ltd. The 3′-UTR of *Lin28a* containing the wild-type (GGAC) motif was amplified from mouse testis cDNA using PCR and then recombining into pmirGLO vector via the ClonExpress One Step Cloning Kit (C112, Vazyme). The 3′-UTR of *Lin28a* containing the mutant (CCTG) motif was synthesized by TsingkeBiotechnology Co., Ltd to ensure precise mutation and incorporated into the pmirGLO vector.

IP-mass spectrometry and co-IP

Human and mouse testes were lysed in Pierce IP Lysis Buffer (88804, Thermo Fisher Scientific) containing complete EDTA-free protease inhibitor cocktail, then immunoprecipitated with anti-IGF2BP1 antibody (22803-1-AP, Proteintech) by a Pierce Crosslink IP Kit (88804, Thermo Fisher Scientific). The immunoprecipitated protein complexes were detected using western blotting. The IGF2BP1 protein complexes pulled down by anti-IGF2BP1 antibody from human and mouse testes were analyzed by the mass spectrometry center of ShanghaiTech University using the entire elutes. HEK-293T cells transfected with pCMV-Myc, pCMV-Myc-ELAVL1, pCMV-3×Flag or pCMV-3×Flag-IGF2BP1 were also lysed with Pierce IP Lysis Buffer and precipitated with anti-Myc or anti-Flag antibodies in the presence or absence of 5 U/μL RNase A. The immunoprecipitated protein complexes were detected using western blotting.

scRNA-seq analysis

Samples from 8-month-old *Igf2bp1* cKO and WT mice were used for scRNA-seq. Detailed scRNA-seq analysis of testicular samples has been described in a previous study[32]. Briefly, individual mouse testicular cells were obtained through enzymatic digestion and loaded on a 10× Genomics chip to form gel beads in emulsion, which were subjected to reverse transcription and PCR amplification, and then sequenced on a Nove-seq 6000 platform (Illumina). A cell-gene expression matrix was obtained with Cell Ranger software (10× Genomics). After quality control, standardization and dimensionality reduction, cell identification and clustering analysis were performed in the R environment. The Seurat FindMarkers function was used for identification of differentially expressed genes in the *Igf2bp1* cKO versus WT A1 cluster groups. GO analysis was performed using WebGestalt 2019 (http://www.webgestalt.org/#).

RIP and sequencing

The process of RIP was carried out using the EZ-Magna RIP kit (17-701, Millipore) in accordance with the manufacturer's guidelines. Briefly, cultured GSCs (~4 ×10^7) or P10 mouse testes (400 mg) were subjected to RIP lysis buffer. The resulting lysates were then centrifuged at 20,000 g for 15 min and the supernatant collected. The supernatant was subsequently used for immunoprecipitation using either anti-IGF2BP1 beads or IgG beads. Both input and co-immunoprecipitated RNAs were isolated using RNA Clean & Concentrator-5 (R1013, Zymo), and were subjected to sequencing (Cloud-Seq Biotech Co., Ltd.) or real-time qPCR analysis. The primers for target mRNAs are listed in Supplementary Data 5.

Western blotting

Both tissues and cultured cells were added to RIPA lysis buffer (P0013B, BiotechWell) for a duration of 30 min on ice. Following centrifugation at 12,000 g for 20 min at 4 °C, the protein concentrations of lysates were measured using a BCA kit (P0012, BiotechWell). SDS-PAGE was

performed with 20 μg of lysate from each sample, and western blottings were carried out in accordance with the previously described protocol[35]. After conducting SDS-PAGE on a 10% gel to load and separate proteins (95 V, 30 min and 120 V, 80 min for loading and separation, respectively), the samples were transferred to 0.45 μm polyvinylidene membranes. The membranes were then blocked with 5% non-fat dried milk, followed by incubation overnight at 4 °C with primary antibodies (Supplementary Data 3) specific for the target proteins. The next day, the membranes were washed with TBS containing 0.1% Tween and incubated with HRP-conjugated secondary antibodies (Supplementary Data 3) for 1 h at room temperature. After washes with TBS 0.1% Tween, the proteins were detected by chemiluminescence (34080, Thermo Fisher Scientific).

RNA extraction and real-time qPCR

The TRIzol method or Total RNA Isolation Kit (RC112-01, Vazyme) were used to extract total RNA from cultured cells or tissues. The quality and concentrations of RNA were assessed using a NanoDrop (840-317400, Thermo Fisher Scientific). Then, 1 μg of extracted RNA was reverse transcribed using a First Strand cDNA Synthesis Kit (K16215, Thermo Fisher Scientific). The cDNAs were used for qRT-PCR in a final 20-μL volume with Power SYBR Green PCR Master Mix in a 96-well thermal cycler. *Gapdh* mRNA expression was used to standardize the expression of target mRNA. The comparative CT (ΔΔCT) method was used to quantify the PCR results. Primers for target mRNAs are listed in Supplementary Data 5.

mRNA stability assay

Huh-6 cells, stably expressing shRNAs targeting IGF2BP1 or a non-specific control (shNS), were seeded into 6-well plates to achieve 50% confluency after 24 h. The cells were then treated with 5 μg/ml actinomycin D (A9415, Sigma-Aldrich) and harvested at specific time points. Total RNA was extracted using the Total RNA Isolation Kit (RC112-01, Vazyme) and analyzed by RT-qPCR.

Luciferase reporter assay

Luciferase plasmids were transfected into cells using Lipofectamine 3000 (L3000001, Thermo Fisher Scientific) according to the manufacturer's protocol. Control and *Igf2bp1* knockdown HEK-293T cells were seeded to reach 70–80% confluency and incubated with the DNA-transfection reagent complexes for 6 h. After incubation, the medium was replaced with fresh growth medium, and cells were further incubated for 48 h. Luciferase activity was determined by a Dual-Glo Luciferase Assay System (Promega, USA) and was shown relative to the control shRNA group.

Statistics and reproducibility

The mean ± standard deviation was used to represent the data unless otherwise specified. For experiments involving multiple treatments, a one-way analysis of variance was conducted to determine significance by GraphPad software. Alternatively, for experiments with only two treatments, Student's *t* test was used to examine statistical significance. $P < 0.05$ was statistically significant. The sample sizes (n numbers) are detailed in the figure legends. Except for scRNA-seq and RIP-seq data, all experiments were independently repeated at least three times. No specific methods were applied for sample allocation into groups. No data were excluded, as all collected data were included in the analysis. Data collection and analysis were performed without blinding to the experimental conditions. For the representative images shown in the paper, each experiment was repeated independently at least three times with consistent results.

Reporting summary

Further information on research design is available in the Nature Portfolio Reporting Summary linked to this article.

Data availability

scRNA-seq data of this study can be found in the NCBI under accession numbers GSE276205. RIP-seq data of this study can be found in the NCBI under accession number GSE275200. Uncropped film data from the western blot can be found in Supplementary Fig. 6 in Supplementary Information. The source data behind the graphs in the paper can be found in Supplementary Data 1.

Received: 22 February 2024; Accepted: 11 October 2024;
Published online: 21 October 2024

References

1. Fayomi, A. P. & Orwig, K. E. Spermatogonial stem cells and spermatogenesis in mice, monkeys and men. *Stem Cell Res.* **29**, 207–214 (2018).
2. Wang, M. et al. Single-Cell RNA Sequencing Analysis Reveals Sequential Cell Fate Transition during Human Spermatogenesis. *Cell Stem Cell* **23**, 599–614.e594 (2018).
3. Mäkelä, J. A. & Hobbs, R. M. Molecular regulation of spermatogonial stem cell renewal and differentiation. *Reproduction* **158**, R169–r187 (2019).
4. Hentze, M. W., Castello, A., Schwarzl, T. & Preiss, T. A brave new world of RNA-binding proteins. *Nat. Rev. Mol. Cell Biol.* **19**, 327–341 (2018).
5. Corley, M., Burns, M. C. & Yeo, G. W. How RNA-Binding Proteins Interact with RNA: Molecules and Mechanisms. *Mol. Cell* **78**, 9–29 (2020).
6. Zhou, Z. et al. RNA Binding Protein Nanos2 Organizes Post-transcriptional Buffering System to Retain Primitive State of Mouse Spermatogonial Stem Cells. *Dev. Cell* **34**, 96–107 (2015).
7. Mikedis, M. M. et al. DAZL mediates a broad translational program regulating expansion and differentiation of spermatogonial progenitors. *Elife* **9**, e56523 (2020).
8. Vikesaa, J. et al. RNA-binding IMPs promote cell adhesion and invadopodia formation. *EMBO J.* **25**, 1456–1468 (2006).
9. Meyer, K. D. & Jaffrey, S. R. Rethinking m(6)A Readers, Writers, and Erasers. *Annu. Rev. Cell Dev. Biol.* **33**, 319–342 (2017).
10. Huang, X. et al. Insulin-like growth factor 2 mRNA-binding protein 1 (IGF2BP1) in cancer. *J. Hematol. Oncol.* **11**, 88 (2018).
11. Weidensdorfer, D. et al. Control of c-myc mRNA stability by IGF2BP1-associated cytoplasmic RNPs. *RNA* **15**, 104–115 (2009).
12. Müller, S. et al. IGF2BP1 enhances an aggressive tumor cell phenotype by impairing miRNA-directed downregulation of oncogenic factors. *Nucleic Acids Res.* **46**, 6285–6303 (2018).
13. Muller, S. et al. The oncofetal RNA-binding protein IGF2BP1 is a druggable, post-transcriptional super-enhancer of E2F-driven gene expression in cancer. *Nucleic Acids Res.* **48**, 8576–8590 (2020).
14. Muller, S. et al. IGF2BP1 promotes SRF-dependent transcription in cancer in a m6A- and miRNA-dependent manner. *Nucleic Acids Res.* **47**, 375–390 (2019).
15. Gu, W., Wells, A. L., Pan, F. & Singer, R. H. Feedback regulation between zipcode binding protein 1 and beta-catenin mRNAs in breast cancer cells. *Mol. Cell Biol.* **28**, 4963–4974 (2008).
16. Stöhr, N. et al. IGF2BP1 promotes cell migration by regulating MK5 and PTEN signaling. *Genes Dev.* **26**, 176–189 (2012).
17. Toledano, H., D'Alterio, C., Czech, B., Levine, E. & Jones, D. L. The let-7-Imp axis regulates ageing of the Drosophila testis stem-cell niche. *Nature* **485**, 605–610 (2012).
18. Hammer, N. A. et al. Expression of IGF-II mRNA-binding proteins (IMPs) in gonads and testicular cancer. *Reproduction* **130**, 203–212 (2005).
19. Brennan, C. M. Steitz JA. HuR and mRNA stability. *Cell Mol. Life Sci.* **58**, 266–277 (2001).
20. Zhang, Z. et al. Activation of ferritinophagy is required for the RNA-binding protein ELAVL1/HuR to regulate ferroptosis in hepatic stellate cells. *Autophagy* **14**, 2083–2103 (2018).
21. Huang, H. et al. Recognition of RNA N(6)-methyladenosine by IGF2BP proteins enhances mRNA stability and translation. *Nat. Cell Biol.* **20**, 285–295 (2018).

22. Rothamel, K. et al. ELAVL1 primarily couples mRNA stability with the 3' UTRs of interferon-stimulated genes. *Cell Rep.* **35**, 109178 (2021).
23. Chen, J. et al. Circular RNA circRHOBTB3 represses metastasis by regulating the HuR-mediated mRNA stability of PTBP1 in colorectal cancer. *Theranostics* **11**, 7507–7526 (2021).
24. Aeckerle, N. et al. The pluripotency factor LIN28 in monkey and human testes: a marker for spermatogonial stem cells? *Mol. Hum. Reprod.* **18**, 477–488 (2012).
25. West, J. A. et al. A role for Lin28 in primordial germ-cell development and germ-cell malignancy. *Nature* **460**, 909–913 (2009).
26. Chakraborty, P. et al. LIN28A marks the spermatogonial progenitor population and regulates its cyclic expansion. *Stem Cells* **32**, 860–873 (2014).
27. Chi, M. N. et al. The RNA-binding protein ELAVL1/HuR is essential for mouse spermatogenesis, acting both at meiotic and postmeiotic stages. *Mol. Biol. Cell* **22**, 2875–2885 (2011).
28. Niimi, Y. et al. Essential role of mouse Dead end1 in the maintenance of spermatogonia. *Dev. Biol.* **445**, 103–112 (2019).
29. Yamaji, M. et al. DND1 maintains germline stem cells via recruitment of the CCR4-NOT complex to target mRNAs. *Nature* **543**, 568–572 (2017).
30. Meng, X. et al. Regulation of cell fate decision of undifferentiated spermatogonia by GDNF. *Science* **287**, 1489–1493 (2000).
31. Nettersheim, D., Jostes, S., Schneider, S. & Schorle, H. Elucidating human male germ cell development by studying germ cell cancer. *Reproduction* **152**, R101–R113 (2016).
32. Zhao, L. et al. Single-cell analysis of developing and azoospermia human testicles reveals central role of Sertoli cells. *Nat. Commun.* **11**, 5683 (2020).
33. Sada, A., Suzuki, A., Suzuki, H. & Saga, Y. The RNA-binding protein NANOS2 is required to maintain murine spermatogonial stem cells. *Science* **325**, 1394–1398 (2009).
34. Zhou, Z., Kawabe, H., Suzuki, A., Shinmyozu, K. & Saga, Y. NEDD4 controls spermatogonial stem cell homeostasis and stress response by regulating messenger ribonucleoprotein complexes. *Nat. Commun.* **8**, 15662 (2017).
35. Yang, C. et al. RNA-binding protein ELAVL2 plays post-transcriptional roles in the regulation of spermatogonia proliferation and apoptosis. *Cell Prolif.* **54**, e13098 (2021).

Acknowledgements

This work was support by grants from National Key Research and Development Program of China (2022YFC2702700); National Natural Science Foundation of China (82171597); Shanghai Hospital Development Center Foundation SHDC12023121; National Natural Science Foundation of China (82201766); Natural Science Foundation of Jiangsu Province (BK20220725).

Author contributions

Y.C.C., L.Z. and Z.Z. designed and conceived the study. L.J.Q., Y.C., X.S., J.Z.Y., Z.Y.X., B.H.W., D.Z.W. and L.J.Y. performed the experiments. H.Y.H., Z.E.L., T.R.H., L.P. and Z.F.J. collected the samples. L.J.Q., Y.C.C. and Y.C. wrote the paper with help from all authors.

Competing interests

The authors declare no competing interests.

Additional information

Supplementary information The online version contains supplementary material available at https://doi.org/10.1038/s42003-024-07055-y.

Correspondence and requests for materials should be addressed to Zhi Zhou, Zheng Li or Chencheng Yao.

Peer review information *Communications Biology* thanks Shuiqiao Yuan and the other, anonymous, reviewer(s) for their contribution to the peer review of this work. Primary Handling Editors: Jun Wei Pek and Christina Karlsson Rosenthal. A peer review file is available.